

MedChemComm

Accepted Manuscript



This article can be cited before page numbers have been issued, to do this please use: R. Bhusal, K. Patel, B. Kwai, A. Swartjes, G. Bashiri, J. Reynisson, J. Sperry and I. K. H. Leung, *Med. Chem. Commun.*, 2017, DOI: 10.1039/C7MD00456G.



This is an Accepted Manuscript, which has been through the Royal Society of Chemistry peer review process and has been accepted for publication.

Accepted Manuscripts are published online shortly after acceptance, before technical editing, formatting and proof reading. Using this free service, authors can make their results available to the community, in citable form, before we publish the edited article. We will replace this Accepted Manuscript with the edited and formatted Advance Article as soon as it is available.

You can find more information about Accepted Manuscripts in the [author guidelines](#).

Please note that technical editing may introduce minor changes to the text and/or graphics, which may alter content. The journal's standard [Terms & Conditions](#) and the ethical guidelines, outlined in our [author and reviewer resource centre](#), still apply. In no event shall the Royal Society of Chemistry be held responsible for any errors or omissions in this Accepted Manuscript or any consequences arising from the use of any information it contains.

Development of NMR and thermal shift assays for the evaluation of *Mycobacterium tuberculosis* isocitrate lyase inhibitors

Ram Prasad Bhusal,¹ Krunal Patel,¹ Brooke X. C. Kwai,^{1,†} Anne Swartjes,^{1,†} Ghader Bashiri,^{2,3} Jóhannes Reynisson,¹ Jonathan Sperry*,¹ and Ivanhoe K. H. Leung*,¹

1. School of Chemical Sciences, The University of Auckland, Private Bag 92019, Victoria Street West, Auckland 1142, New Zealand.

2. School of Biological Sciences, The University of Auckland, Private Bag 92019, Victoria Street West, Auckland 1142, New Zealand.

3. Maurice Wilkins Centre for Molecular Biodiscovery, The University of Auckland, Private Bag 92019, Victoria Street West, Auckland 1142, New Zealand.

† These authors contributed equally to this work.

Abstract

The enzymes isocitrate lyase (ICL) isoforms 1 and 2 are essential for *Mycobacterium tuberculosis* survival within macrophages during latent tuberculosis (TB). As such, ICLs are attractive therapeutic targets for the treatment of tuberculosis. However, there are few biophysical assays that are available for accurate kinetic and inhibition studies of ICL *in vitro*. Herein we report the development of a combined NMR spectroscopy and thermal shift assay to study ICL inhibitors for both screening and inhibition constant (IC₅₀) measurement. Operating this new assay in tandem with virtual high-throughput screening has led to the discovery of several new ICL1 inhibitors.

Keywords

Tuberculosis; Isocitrate lyase; NMR spectroscopy; Enzyme inhibition; Virtual screening

Introduction

Tuberculosis (TB) is a high burden infectious disease that is caused by *Mycobacterium tuberculosis*.^{1,2} In 2015, there were over 10 million new TB cases and around 1.8 million TB-related deaths.³ TB has a long latency period; once a human is infected with *M. tuberculosis*, the bacteria may stay inactive within macrophages for many years leading to a syndrome that is known as latent TB.⁴⁻⁶ The environment inside macrophages is relatively hypoxic and lacking in external nutrients. In order to survive under these conditions, *M. tuberculosis* is able to simultaneously catabolise different carbon sources, including fatty acids and cholesterol that are available in relative abundance inside macrophages.⁷⁻⁹ The enzymes isocitrate lyase (ICL) isoforms 1 and 2 play essential roles in this metabolic adaptation.¹⁰ ICLs are key enzymes in both the *M. tuberculosis* glyoxylate and methylcitrate cycles. In the glyoxylate cycle, ICLs catalyse the conversion of the tricarboxylic acid (TCA) cycle intermediate isocitrate into glyoxylate and succinate (Figure 1a), thus bypassing the two decarboxylation steps in the TCA cycle and preserving these carbons for gluconeogenesis.^{11,12} In the methylcitrate cycle, ICLs catalyse the conversion of methylisocitrate, an intermediate of the propionate degradation pathway, to pyruvate and succinate. Propionate, which is toxic to the bacteria, is generated by β -oxidation of odd chain fatty acids and cholesterol that *M. tuberculosis* may utilise as carbon sources.^{12,13}

Given the pivotal roles ICLs play in the survival of *M. tuberculosis* inside macrophages, ICLs are attractive inhibition targets for the treatment of latent TB.¹⁴⁻¹⁶ We recently instigated a research programme aimed at identifying new inhibitors of ICLs, but it was readily apparent that few accurate biophysical assays are available to study ICL kinetics and inhibition *in vitro*. Most ICL assays rely on ultraviolet/visible (UV/vis) spectrophotometry to determine the amount of glyoxylate that is formed as a result of ICL-catalysed reactions. For example,

one method uses lactate dehydrogenase (LDH) to catalyse the reduction of glyoxylate to glycolate, during which NADH (a cosubstrate of LDH) is oxidised to NAD⁺. The decrease in NADH concentration is then measured by UV/vis spectrophotometry using a tetrazolium/formazan dye.¹⁷ Another method relies on the reaction phenylhydrazine with glyoxylate to form a hydrazone, which is subsequently analysed by UV/vis spectrophotometry.¹⁸ In addition to kinetic assays, the use of native non-denaturing mass spectrometry and intrinsic protein fluorescence to monitor ICL-inhibitor binding interactions have also been reported.¹⁹ However, these assays have several drawbacks. Auto-oxidation of NADH to NAD⁺ may affect the accuracy of the LDH-coupled assay.²⁰ In addition, this method is not suitable for measuring the methylisocitrate lyase activity of ICLs because of LDH cannot take pyruvate as substrate.²⁰ For the phenylhydrazine-coupled assay, the accuracy of the assay may be compromised by the rate of the glyoxylate-phenylhydrazone complex formation, which is pH dependent and gets slower above pH 7.^{21,22} Phenylhydrazine is also unstable at pH 7 and above, the breakdown products may lead to a slow increase in the UV absorption, thus affecting the accuracy of the measurements.^{21,22}

¹H nuclear magnetic resonance (NMR) spectroscopy is an established technique for the study of enzyme kinetics that has been used to characterise different enzyme systems including (but not limited to) carbohydrate-processing enzymes,^{23,24} enzymes related to antibiotic resistance²⁵ and oxygenases.^{26,27} ¹H NMR spectroscopy enables the direct monitoring of reaction kinetics in real time and accurate, quantitative information can be obtained by following changes in the peak area of the resonances associated with the substrate and/or reaction product(s). In contrast, thermal shift assay is a simple and high-throughput method that can be used to study protein-ligand binding interactions by measuring the melting temperature of a protein by the use of a fluorescence dye that is sensitive to changes in hydrophobic environment.^{28–30} When a protein unfolds, it exposes its hydrophobic core. This

enables the dye to bind to the exposed hydrophobic regions, which lead to fluorescence. Ligand binding may stabilise or destabilise the protein towards thermal denaturation, leading to a positive or negative shift in the protein's melting temperature.^{31,32} We reasoned that a strategy that combined ¹H NMR spectroscopy and a thermal shift assay would provide a good way to accurately monitor ICL kinetics and inhibition. By using *M. tuberculosis* ICL1 as a model system, we have optimised the experimental conditions and demonstrated the feasibility of applying a joint NMR and thermal shift strategy for inhibitor screening, inhibition constant (IC₅₀) measurement and for elucidating the modes of action of ICL inhibitors. Finally, this technique is exemplified by work in tandem with virtual high-throughput screening, which subsequently led to the discovery of several novel ICL1 inhibitors. ICL2 was not used in this study because it was reported to be unstable *in vitro*¹⁷ and it possesses relatively low catalytic activity when compared to ICL1.¹²

Results and Discussion

ICL1 enzyme kinetics by ¹H NMR

We first tested the use of ¹H NMR spectroscopy to monitor the ICL1-catalysed turnover of isocitrate to succinate and glyoxylate. DL-Isocitrate, which is available commercially, was used as the substrate. MgCl₂ was added to the reaction mixture as it was previously shown to be important for ICL1 activity.¹⁷ ¹H spectra were recorded at ~1.3 minute intervals. Upon addition of the enzyme, the peaks corresponding to isocitrate dropped in intensity, which was accompanied by the appearance of a new singlet peak at 2.3 ppm, corresponding to succinate (Figure 1b). Integration of the isocitrate and succinate peaks showed that the reaction appeared to slow down when ~50% of the isocitrate was consumed (Figure 1c). As the isocitrate was a racemic mixture, this result infers that ICL1 has a preference for one

enantiomer, which is in agreement with a previous study that showed D-isocitrate is the preferred substrate of the enzyme.³³

Divalent metals play important role for the activity of ICL1. Previous studies showed that Mg^{2+} (and to a lesser extent, Mn^{2+}) are required for optimal ICL1 activity.^{17,34} In order to confirm the concentration of divalent magnesium that is required for optimal activity of the enzyme, the reaction was run using different concentrations of $MgCl_2$. Under our reaction conditions, 500 μM of $MgCl_2$ was required for the optimal activity (Supplementary Figure S1). At least 500 μM of $MgCl_2$ was used in all subsequent kinetic and inhibition assays.

The kinetic parameters for ICL1 with DL-isocitrate were then evaluated by 1H NMR. The Michaelis constant (K_M) was found to be $290 \pm 10 \mu M$ and the catalytic constant (k_{cat}) was determined to be $4.3 \pm 0.1 s^{-1}$ (Supplementary Figure S2). These values were similar to those obtained by Gould *et al.* using the aforementioned LDH assay, which were 190 μM and 5.24 s^{-1} respectively (Table 1).¹² The slight discrepancy between the two measurements is likely due to differences in the reaction conditions. Overall, this validated the accuracy of our 1H NMR assay to study ICL1 kinetics.

We then tested the use of 1H NMR spectroscopy to monitor the ICL1-catalysed turnover of methylisocitrate to pyruvate and succinate (Supplementary Figure S3a). (2S,3R)-2-methylisocitrate was used as substrate. In the presence of ICL1 and Mg^{2+} , two new singlet signals at ~ 2.3 ppm, one corresponded to succinate and the other corresponded to pyruvate, were found to increase in intensity over time (Supplementary Figure S3b). This was coupled with a drop in intensity of the methylisocitrate signals. We then repeated the experiments at different methylisocitrate concentrations. Interestingly, substrate inhibition was observed when methylisocitrate concentration exceeded 1 mM (Supplementary Figure S4). Substrate inhibition was not observed when isocitrate was used as substrate. Further investigations are

required to fully understand the biological significance of these observations. Overall, our results showed that ^1H NMR spectroscopy is a versatile and informative tool to study ICL1 kinetics that allows the use of different substrates and enables kinetic information to readily be measured and quantified.

Inhibition studies of ICL1 by ^1H NMR

We then applied our new NMR-based assay to study ICL1 inhibition. Initially, we chose four known ICL inhibitors, including three so-called first generation inhibitors itaconic acid,³⁵ 3-nitropropionate³⁶ and 3-bromopyruvate.³⁷ Itaconic acid and 3-nitropropionate are noncovalent inhibitors of ICL1 whereas 3-bromopyruvate inhibits ICL1 in a covalent manner. Methyl 4-(4-methoxyphenyl)-4-oxobut-2-enoate, an inhibitor that was discovered last year by Liu *et al.* using high-throughput screening, was also evaluated (Table 2).³⁸

Single concentration inhibition experiments were first conducted (Supplementary Figure S5). In agreement with previous studies,¹⁷ our ^1H NMR assay showed that 3-nitropropionate was the most potent inhibitor amongst 3-nitropropionate, 3-bromopyruvate and itaconic acid. Under our assay condition, methyl 4-(4-methoxyphenyl)-4-oxobut-2-enoate was the weakest of the four tested. We then repeated our measurements at different inhibitor concentrations in order to obtain quantitative inhibition information (IC_{50} ; Table 2 and Supplementary Figures S6–S9). The IC_{50} values of 3-nitropropionate, 3-bromopyruvate, itaconic acid and methyl 4-(4-methoxyphenyl)-4-oxobut-2-enoate were found to be $14.7 \pm 1.8 \mu\text{M}$, $17.5 \pm 1.0 \mu\text{M}$, $29.4 \pm 4.1 \mu\text{M}$ and $250 \pm 7 \mu\text{M}$ respectively. The reported IC_{50} value for methyl 4-(4-methoxyphenyl)-4-oxobut-2-enoate was $30.9 \mu\text{M}$.³⁸ The slight discrepancy in our measured and reported IC_{50} values for methyl 4-(4-methoxyphenyl)-4-oxobut-2-enoate is likely due to the different reaction conditions and assays used in the two studies. Overall, our results show

that ^1H NMR is a useful tool to study ICL1 inhibition *in vitro*, enabling a rapid evaluation of inhibitor strength as well as providing quantitative information such as IC_{50} .

Thermal shift assay to study ICL1-inhibitor interactions

Although ^1H NMR spectroscopy was found to be a useful method to study ICL1 inhibition, it is relatively low throughput and labour intensive. A high throughput assay is needed to facilitate the efficient screening and development of new ICL inhibitors. Thermal shift assays are a widely-used method to study protein-ligand interactions.^{28–30} The principle of a thermal shift assay is based on the premise that ligand binding can stabilise or destabilise protein to thermal denaturing, and therefore lead to a shift in the protein's melting temperature.

First, the melting temperature of ICL1 was measured. As MgCl_2 is important for the activity of the enzyme, a saturating concentration of 1 mM was used. The melting temperature of ICL1 in the presence of MgCl_2 was found to be 43.0 °C. Next, the melting temperatures of ICL1 in the presence of a saturating concentration (1 mM) of the aforementioned inhibitors and MgCl_2 were measured. Addition of 3-bromopyruvate or itaconic acid were found to stabilise ICL1, with positive shifts to melting temperatures of 52.5 °C and 53.3 °C respectively. Interestingly, 3-nitropropionate and methyl 4-(4-methoxyphenyl)-4-oxobut-2-enoate were found to destabilise the protein, with negative thermal shifts to 40.9 °C and 37.6 °C respectively (Supplementary Figure S10).

A negative thermal shift upon ligand binding has been previously observed for other protein systems.^{31,32} A positive thermal shift may be observed if the ligand induces the protein to adapt a more stable 'closed' conformation, whilst negative thermal shift may be observed if the ligand keeps the protein in a less stable 'open' conformation. Previous structural studies by Sharma *et al.* showed that ICL1 may undergo a two-step conformation change upon substrate binding (Supplementary Figure S11).³⁹ Indeed, a crystal structure of ICL1 in the

presence of both 3-nitropropionate and glyoxylate was found to adapt a 'closed' conformation (PDB id: 1F8I). 3-Nitropropionate is a structural analogue of succinate.³⁶ We reasoned that the binding of 3-nitropropionate on its own may keep ICL1 in the open conformation in order to allow glyoxylate to bind. However, in the presence of both 3-nitropropionate and glyoxylate, the protein can then undergo conformational change to the 'closed' conformation, as suggested by the crystal structure, to catalyse the reverse reaction. This proposal is consistent with the mechanism suggested by Sharma *et al.*³⁹ It should also be noted that binding of 3-nitropropionate or methyl 4-(4-methoxyphenyl)-4-oxobut-2-enoate may induce a change in the oligomeric state of ICL1, which exists as a tetramer in solution.³⁹ However, based on evidence from X-ray crystallography³⁹ and molecular docking,³⁸ both compounds are not known to bind at the oligomerisation interface between the ICL1 monomers, or interfere with the residues that were previously identified as important for the protein's oligomerisation.⁴⁰

Application of the combined ¹H NMR and thermal shift assays with virtual high-throughput screening

Virtual high-throughput screening is a cost-effective and efficient strategy to identify chemical structures that are potentially important for binding to a target protein.⁴¹⁻⁴³ Obviously, the hits identified by virtual high-throughput screening needed to be verified experimentally. In order to test the applicability of the ¹H NMR and thermal shift assays and to identify new inhibitors of ICL1, a virtual screen was conducted. Using the crystal structure of ICL1 (PDB ID: 1F8I, resolution 2.25 Å),³⁹ a screen was performed with the InterBioScreen Ltd natural product collection.⁴⁴ 9050 compounds were screened and four different scoring functions, including GoldScore (GS),⁴⁵ ChemScore (CS),^{46,47} Piecewise Linear Potential (ChemPLP)⁴⁸ and Astex Statistical Potential (ASP),⁴⁹ were used. Ten

docking runs were allowed for each compound with virtual screening setting (30%). Based on the scores, ligands with predicted low GS (<45), CS (<20), ChemPLP (<45), ASP (<20) as well as those with no hydrogen bonding (HB=0) were eliminated, which resulted in 840 compounds. These compounds were screened again with high search efficiency (100%) and fifty docking runs. Candidates with low GS (<38), CS (<17), ChemPLP (<38), ASP (<17) as well as those with predicted limited hydrogen bonding (HB<1) were eliminated, resulting in 205 candidates. For both rounds of screening the cut-off values of the scores were determined based on the scores of the known inhibitors itaconic acid, 3-nitropropionate and 3-bromopyruvate. Furthermore, only compounds with predicted hydrogen bonding were taken forward since hydrogen bond is important not only for the affinity but also the specificity of the ligand binding.⁵⁰ These candidates were then visually inspected for consensus of the best predicted configuration of the ligands between the scoring functions. Ligands that showed plausible configurations, i.e., not strained, lipophilic moieties not pointing into the water environment resulting in an entropy penalty, were taken forward. Furthermore, compounds that did not contain undesirable moieties that are linked to general cell toxicity (e.g. thiourea and aliphatic ketones) and chemical reactivity (e.g. Michael acceptors and imines), were chosen.^{51,52} This screening methodology has been successfully applied previously to find active ligands for various biomolecular systems.^{53–56} In total, 41 compounds were selected for experimental testing (Supplementary Figure S12 and Supplementary Table S1).

We then applied the ¹H NMR and thermal shift assays to verify the hits obtained from the virtual screen. First, we tested the compounds using the thermal shift assay. Out of the 41 compounds, 19 induced a shift of more than 0.5 °C (positive or negative) in the melting temperature of ICL (Supplementary Figure S13). This was followed with ¹H NMR-based single concentration inhibition experiment to test the 19 hits. The result showed that two molecules significantly inhibited ICL1 (Compounds **29** and **38**, Supplementary Figure S14).

The IC_{50} of the molecules were both $>100 \mu\text{M}$ (Supplementary Figures S15–S16 and Table 2). Molecular modelling suggests compounds **29** and **38** both occupy the substrate and Mg^{2+} binding sites. The reason for the relatively low IC_{50} values is due to the removal of the Mg^{2+} ion from the binding pocket upon inhibitor binding. Mg^{2+} sits within a cavity that is predicted to be occupied by aliphatic moieties of the inhibitors. Thus, the inhibitors need to displace the magnesium ion to bind efficiently, which would require a considerable energy expenditure due to the saturation concentration (5 mM) of the ion in the experimental setup. The main stream molecular descriptors (molecular weight, log P, hydrogen bond donors / acceptors, polar surface area and rotatable bonds see Supplementary Table S2) for compounds **29** and **38** were calculated and they conform to drug-like chemical space except Log P and numbers of hydrogen bond donors, which are in lead-like chemical space (for the definition of chemical space see reference 57). Furthermore, the molecular weight for the hits is in the low to mid 300s, making them excellent starting points for chemical modification and further development. Finally, nine close structural derivatives were purchased to generate a structural activity (SAR) profile (Supplementary Figure S17), but none showed any activity. In general, docking to the binding site showed that these compounds are too bulky to fit into it. Overall, our results show that combining ^1H NMR and thermal shift assays is an effective strategy for screening potential ICL1 inhibitors.

Conclusions

ICL isoforms 1 and 2 are important enzymes for the survival of *M. tuberculosis* in macrophages, enabling the bacteria to utilise fatty acids and cholesterol as carbon sources. ICLs are attractive inhibition targets for the treatment of latent TB. By using ICL1 as a model system, we have demonstrated the general applicability of a combined ^1H NMR and thermal shift assays to screen for and evaluate ICL inhibitors. Both methods presented herein are

relatively simple to carry out. In contrast to current fluorescence-based assays that rely on enzyme or chemically coupled reactions, the NMR assay described herein enables a direct observation of substrate consumption and product formation and is therefore less prone to errors. One minor drawback of the NMR assay is the low throughput associated with monitoring reactions in real time. Typically, around 15 to 20 minutes of measurement time (six to eleven ^1H experiments) was needed to obtain an initial rate. This equates to around seven hours of total measurement time to obtain a full kinetic analysis or a complete IC_{50} curve with, for example, six concentration points in triplicate. In contrast, the thermal shift assay is a high-throughput method enabling semi-automatic measurements using multi-well plates. Ligand binding to ICL1 was easily identified through a change in the protein's melting temperature. Interestingly, we observed both positive (i.e. stabilising) and negative (i.e. destabilising) thermal shifts of ICL1 with four known inhibitors, likely due to the inhibitors keeping ICL1 in either the open or closed conformations. We have demonstrated the utility of these assays by validating a small library of compounds that were obtained by a virtual high-throughput screen. This ultimately led to the discovery of two novel ICL1 inhibitors that are the subject of ongoing medicinal chemistry studies in our laboratories.

Experimental section

Materials

Unless otherwise stated, all chemicals were purchased from Sigma-Aldrich/Merck, Thermo Fisher Scientific, Environmental Control Products (ECP), AK Scientific, Global Science - a VWR/Bio-Strategy Company and Bio-Rad. Tris- D_{11} and D_2O were from Cambridge Isotope Laboratories or Cortecnet. Restriction enzymes *Bsa*I-HF and T4 DNA polymerase were obtained from New England Biolabs. Competent cells XL10-Gold and BL21 (DE3) were obtained from Agilent. The Bio-Rad Precision Plus Protein Kaleidoscope Prestained Protein

Standards were used for sodium dodecylsulphate polyacrylamide gel electrophoresis (SDS-PAGE). Methyl 4-(4-methoxyphenyl)-4-oxobut-2-enoate was obtained from Enamine. Compounds from virtual screening were obtained from InterBioScreen.

Cloning of ICL1

Synthetic gene (gBlocks) encoding *M. tuberculosis* ICL1 (Supplementary Table S3) were obtained from Integrated DNA Technologies. The pNIC28-Bsa4 vector was a gift from Opher Gileadi (Addgene plasmid #26103).⁵⁸ In order to clone onto the pNIC28-Bsa4 vector, the tacttccaatccatg sequence was added to the 5' end and taacagtaaaggaggata was added to the 3' end of the DNA sequence encoding *M. tuberculosis* ICL1 (Supplementary Table S3) when designing the synthetic gene. The synthetic gene and the pNIC28-Bsa4 vector were prepared and cloned using the procedure reported by Gileadi *et al.* with XL10-Gold.⁵⁹ The recombinant plasmid was confirmed by DNA sequencing (DNA Sequencing Centre, The University of Auckland). The correct plasmid were then used to transform BL21 (DE3) competent cells for protein expression.

Production and purification of ICL1

The recombinant plasmid was first transformed in *E. coli* BL21(DE3). Starter culture was incubated overnight at 37 °C with shaking in 2YT media. The starter culture was then diluted with fresh 2YT media, which was then incubated at 37 °C with shaking until OD₆₀₀ of 0.6. Isopropyl-β-D-thiogalactopyranoside (IPTG; 200 μM final concentration) was then added and further incubated at 18 °C with shaking for a further 16 to 20 hours. Cells were harvested by centrifugation. Cell pellets were obtained by centrifugation and resuspended in 50 mM HEPES buffer pH 7.8 with 5 mM imidazole and 500 mM NaCl. The cells were lysed on ice by sonication (4 x 20 seconds) burst at 60% amplitude with 40 seconds rest in between. The

protein was purified by 5 mL His-trap column eluting with Tris-HCl buffer pH 7.8 with 500 mM imidazole and followed by gel filtration using 50 mM Tris-HCl buffer pH 7.5.

Thermal shift assay

Thermal shift assay was carried out using a BioRad MyiQ real time PCR instrument. The assay was carried out using 20 μ M ICL1, 1 mM compounds and 1 mM MgCl_2 in 50 mM Tris-HCl pH 7.5. Protein unfolding was monitored by measuring the fluorescence of the SYPRO Orange dye. The dye stock (5000x concentrate) was first diluted in 50 mM Tris-HCl (pH 7.5) to a 200x concentrate before diluting by 5 times into the sample. Temperature was increased from 25 to 95 $^{\circ}\text{C}$ at 1 $^{\circ}\text{C}$ increment every 60 seconds. All measurements were performed in triplicate. For determination of protein melting temperature values, melting curve for each data set was analysed by SigmaPlot 13 (USA) and fitted with the *Sigmoid, 3 parameter* model.

NMR experiments

NMR experiments were conducted at a ^1H frequency of 500 MHz using a Bruker Avance III HD spectrometer equipped with a BBFO probe. Experiments were conducted at 300 K. Standard 5 mm NMR tubes (Wilmad) using a sample volume of 500 μL were used in all experiments. The pulse tip-angle calibration using the single-pulse nutation method (Bruker *pulsecal* routine) was undertaken for each sample.⁶⁰ All measurements were performed in triplicate.

Time course experiments were monitored by standard Bruker ^1H experiments with water suppression by excitation sculpting. Unless otherwise stated, the number of transients was 16, and the relaxation delay was 2 seconds. The lag time between addition of enzyme and the end of the first experiment was usually 4 minutes. Initial rates were calculated by linear fitting

using Excel 2013 (Microsoft) for data points up to 20% turnover. Kinetic parameters were obtained using the Hanes plot. Linear fitting was done using Excel 2013 (Microsoft). All NMR samples contained 190 nM ICL1, 1 mM DL-isocitrate and 5 mM MgCl₂ buffered with 50 mM Tris-D₁₁ (pH 7.5) in 90% H₂O and 10% D₂O. For kinetic parameter measurements, the isocitrate concentrations ranged from 50 μM to 750 μM. For single concentration inhibition assay, 100 μM inhibitors was used. For IC₅₀ measurements, varying concentrations of inhibitors were used. IC₅₀ values were obtained by SigmaPlot 13 and fitted with the *Sigmoid, 3 parameter* model.

Virtual high throughput screening

The compounds were docked to the crystal structure of ICL I (PDB ID: 1F8I),³⁹ which was obtained from the Protein Data Bank (PDB).^{61,62} The Scigress version FJ 2.6 program (Scigress: Version FJ 2.6 (EU 3.1.7; (Fijitsu Limited, 2008-2016)) was used to prepare the crystal structure for docking, i.e., hydrogen atoms added, the co-crystallised succinic acid and glyoxylic acid were removed from protein, the magnesium ion as well as crystallographic water molecules. The Scigress software suite was also used to transfer the structures from 2d to 3D followed by structural optimisation using the MM2 force field.⁶³ The centre of the binding was defined on the co-crystallised ligand with coordinates (x = 5.931, y = 56.950, z = 83.843) with 10 Å radius. For the initial screen 30% search efficiency was used (virtual screen) with ten runs per compound. For the second phase (re-dock) 100% efficiency was used in conjunction with fifty docking runs. The GoldScore,⁴⁵ ChemScore,^{46,47} ChemPLP⁴⁸ and ASP⁴⁹ scoring functions were implemented to validate the predicted binding modes and relative energies of the ligands using GOLD v5.2 software suite. The InterBioScreen Ltd natural product collection was used for the screening.⁴⁴ The robustness of the protocol was tested by re-docking the co-crystallised ligand (succinic acid) with these results: RMSD

(root-mean-square deviation) GS – 1.750 Å, CS – 0.929 Å, PLP – 0.747 Å and ASP – 1.882 Å, verifying the validity of the procedure. The QikProp v3.21 (QikProp v3.2, Schrödinger, New York, 3.2, 2009.) software package was used to calculate the molecular descriptors of the compounds. The reliability of the prediction power of QikProp is established for the molecular descriptors used in this study.⁶⁴

Synthesis of (2S,3R)-2-methylisocitrate

(2S,3R)-2-methylisocitrate was prepared according to the procedure reported by Darley *et al.*⁶⁵

Acknowledgement

We thank the University of Auckland for a Doctoral Scholarship (R.P.B) and the Maurice and Phyllis Paykel Trust for funding. G.B. is supported by a Sir Charles Hercus Fellowship awarded through the Health Research Council of New Zealand. We thank Professor Bernard Golding (Newcastle University, UK) for his advice when preparing (2S,3R)-2-methylisocitrate. We thank Dr M. Schmitz for maintenance of the NMR facility and Ms K. Boxen for the DNA sequencing service.

Conflict of Interest

The authors declare no competing interests.

References

1. Pai, M.; Behr, M. A.; Dowdy, D.; Dheda, K.; Divangahi, M.; Boehme, C. C.; Ginsberg, A.; Swaminathan, S.; Spigelman, M.; Getahun, H.; Menzies, D.; Raviglione, M. Tuberculosis. *Nat. Rev. Dis. Primers* **2016**, *27*, 16076.

2. Zumla, A.; Raviglione, M.; Hafner, R.; von Reyn, C. F. Tuberculosis. *N. Engl. J. Med.* **2013**, *368*, 745–755.
3. World Health Organization, Regional Office for South-East Asia. *Bending the curve – ending TB: Annual report 2017*; New Delhi, 2017.
4. Getahun, H.; Matteelli, A.; Chaisson, R. E.; Raviglione, M. Latent *Mycobacterium tuberculosis* infection. *N. Engl. J. Med.* **2015**, *372*, 2127–2135.
5. Esmail, H.; Barry, C. E.; Young, D. B.; Wilkinson, R. J. The ongoing challenge of latent tuberculosis. *Phil. Trans. R. Soc. B* **2014**, *369*, 20130437.
6. Lin, P. L.; Flynn, J. L. Understanding latent tuberculosis: a moving target. *J. Immunol.* **2010**, *185*, 15–22.
7. de Carvalho, L. P. S.; Fischer, S. M.; Marrero, J.; Nathan, C.; Ehrh, S.; Rhee, K. Y. Metabolomics of *Mycobacterium tuberculosis* reveals compartmentalized co-catabolism of carbon substrates. *Chem. Biol.* **2010**, *17*, 1122–1131.
8. Russell, D. G.; VanderVen, B. C.; Lee, W.; Abramovitch, R. B.; Kim, M.-J.; Homolka, S.; Niemann, S.; Rohde, K. H. *Mycobacterium tuberculosis* wears what it eats. *Cell Host Microbe* **2010**, *8*, 68–76.
9. Schnappinger, D.; Ehrh, S.; Voskuil, M. I.; Liu, Y.; Mangan, J. A.; Monahan, I. M.; Dolganov, G.; Efron, B.; Butcher, P. D.; Nathan, C.; Schoolnik, G. K. Transcriptional adaptation of *Mycobacterium tuberculosis* within macrophages: insights into the phagosomal environment. *J. Exp. Med.* **2003**, *198*, 693–704.
10. Muñoz-Elías, E. J.; McKinney, J. D. *Mycobacterium tuberculosis* isocitrate lyases 1 and 2 are jointly required for in vivo growth and virulence. *Nat. Med.* **2005**, *11*, 638–644.
11. McKinney, J. D.; Höner zu Bentrup, K.; Muñoz-Elías, E. J.; Miczak, A.; Chen, B.; Chan, W. T.; Swenson, D.; Sacchetti, J. C.; Jacobs Jr, W. R.; Russell, D. G. Persistence of

- Mycobacterium tuberculosis* in macrophages and mice requires the glyoxylate shunt enzyme isocitrate lyase. *Nature* **2000**, *406*, 735–738.
12. Gould, T. A.; Van De Langemheen, H.; Muñoz-Eliás, E. J.; McKinney, J. D.; Sacchettini, J. C. Dual role of isocitrate lyase 1 in the glyoxylate and methylcitrate cycles in *Mycobacterium tuberculosis*. *Mol. Microbiol.* **2006**, *61*, 940–947.
13. Eoh, H.; Rhee, K. Y. Methylcitrate cycle defines the bactericidal essentiality of isocitrate lyase for survival of *Mycobacterium tuberculosis* on fatty acids. *Proc. Natl. Acad. Sci. U.S.A.* **2014**, *111*, 4976–4981.
14. Bhusal, R. P.; Bashiri, G.; Kwai, B. X. C.; Sperry, J.; Leung, I. K. H. Targeting isocitrate lyase for the treatment of latent tuberculosis. *Drug Discov. Today* **2017**, *22*, 1008–1016.
15. Krátký, M.; Vinšová, J. Advances in mycobacterial isocitrate lyase targeting and inhibitors. *Curr. Med. Chem.* **2012**, *19*, 6126–6137.
16. Lee, Y. V.; Wahab, H. A.; Choong, Y. S. Potential inhibitors for isocitrate lyase of *Mycobacterium tuberculosis* and non-*M. tuberculosis*: a summary. *BioMed Res. Int.* **2015**, *2015*, 895453.
17. Höner Zu Bentrup, K.; Miczak, A.; Swenson, D. L.; Russell, D. G. Characterization of activity and expression of isocitrate lyase in *Mycobacterium avium* and *Mycobacterium tuberculosis*. *J. Bacteriol.* **1999**, *181*, 7161–7167.
18. Dixon, G. H.; Kornberg, H. L. Assay methods for key enzymes of the glyoxylate cycle. *Proc. Biochem. Soc.* **1959**, *72*, 3p.
19. Pham, T. V.; Murkin, A. S.; Moynihan, M. M.; Harris, L.; Tyler, P. C.; Shetty, N.; Sacchettini, J. C.; Huang, H.-l.; Meek, T. D. Mechanism-based inactivator of isocitrate lyases 1 and 2 from *Mycobacterium tuberculosis*. *Proc. Natl. Acad. Sci. U.S.A.* **2017**, *114*, 7617–7622.

20. Chenault, H. K.; Whitesides, G. M. Lactate dehydrogenase-catalyzed regeneration of NAD from NADH for use in enzyme-catalyzed synthesis. *Bioorg. Chem.* **1989**, *17*, 400–409.
21. Vanni, P.; Giachetti, E.; Pinzauti, G.; Mcfadden, B. A. Comparative structure, function and regulation of isocitrate lyase, an important assimilatory enzyme. *Comp. Biochem. Physiol.* **1990**, *95B*, 431–458.
22. Lui, N. S. T.; Roels, O. A. An improved method for determining glyoxylic acid. *Anal. Biochem.* **1970**, *38*, 202–209.
23. Tyl, C.; Felsing, S.; Brecker, L. In situ proton NMR of glycosidase catalyzed hydrolysis and reverse hydrolysis. *J. Mol. Catal. B. Enzym.* **2004**, *28*, 55–63.
24. Spangenberg, P.; Chiffolleau-Giraud, V.; André, C.; Dion, M.; Rabiller, C. Probing the transferase activity of glycosidases by means of in situ NMR spectroscopy. *Tetrahedron Asymmetry* **1999**, *10*, 2905–2912.
25. van Berkel, S. S.; Nettleship, J. E.; Leung, I. K. H.; Brem, J.; Choi, H.; Stuart, D. I.; Claridge, T. D. W.; McDonough, M. A.; Owens, R. J.; Ren, J.; Schofield, C. J. Binding of (5S)-penicilloic acid to penicillin binding protein 3. *ACS Chem. Biol.* **2013**, *8*, 2112–2116.
26. Leung, I. K. H.; Krojer, T. J.; Kochan, G. T.; Henry, L.; von Delft, F.; Claridge, T. D. W.; Oppermann, U.; McDonough, M. A.; Schofield, C. J. Structural and mechanistic studies on γ -butyrobetaine hydroxylase. *Chem. Biol.* **2010**, *17*, 1316–1324.
27. Mbenza, N. M.; Vadakkedath, P. G.; McGillivray, D. J.; Leung, I. K. H. NMR studies of the non-haem Fe(II) and 2-oxoglutarate-dependent oxygenases. *J. Inorg. Biochem.* **2017**, in press.
28. Pantoliano, M. W.; Petrella, E. C.; Kwasnoski, J. D.; Lobanov, V. S.; Myslik, J.; Graf, E.; Carver, T.; Asel, E.; Springer, B. A.; Lane, P.; Salemme, F. R. High-density miniaturized

- thermal shift assays as a general strategy for drug discovery. *J. Biomol. Screen.* **2001**, *6*, 429–440.
29. Zhang, R.; Monsma, F. Fluorescence-based thermal shift assays. *Curr. Opin. Drug Discov. Dev.* **2010**, *13*, 389–402.
30. Lo, M.-C.; Aulabaugh, A.; Jin, G.; Cowling, R.; Bard, J.; Malamas, M.; Ellestad, G. Evaluation of fluorescence-based thermal shift assays for hit identification in drug discovery. *Anal. Biochem.* **2004**, *332*, 153–159.
31. Matulis, D.; Kranz, J. K.; Salemme, F. R.; Todd, M. J. Thermodynamic stability of carbonic anhydrase: measurements of binding affinity and stoichiometry using ThermoFluor. *Biochemistry* **2005**, *44*, 5258–5266.
32. Cimperman, P.; Baranauskiene, L.; Jachimoviciūte, S.; Jachno, J.; Torresan, J.; Michailoviene, V.; Matuliene, J.; Sereikaite, J.; Bumelis, V.; Matulis, D. A quantitative model of thermal stabilization and destabilization of proteins by ligands. *Biophys J.* **2008**, *95*, 3222–3231.
33. Smith, R. A.; Gunsalus, I. C. Isocitritase: enzyme properties and reaction equilibrium. *J. Biol. Chem.* **1957**, *229*, 305–319.
34. Giachetti, E.; Vanni, P. Effect of Mg^{2+} and Mn^{2+} on isocitrate lyase, a non-essentially metal-ion-activated enzyme. A graphical approach for the discrimination of the model for activation. *Biochem J.* **1991**, *276*, 223–230.
35. McFadden, B. A.; Purohit, S. Itaconate, an isocitrate lyase directed inhibitor in *Pseudomonas indigofera*. *J. Bacteriol.* **1977**, *131*, 136–144.
36. Schloss, J. V.; Cleland, W. W. Inhibition of isocitrate lyase by 3-nitropropionate, a reaction-intermediate analogue. *Biochemistry* **1982**, *21*, 4420–4427.
37. Ko, Y. H.; McFadden, B. A. Alkylation of isocitrate lyase from *Escherichia coli* by 3-bromopyruvate. *Arch. Biochem. Biophys.* **1990**, *278*, 373–380.

38. Liu, Y.; Zhou, S.; Deng, Q.; Li, X.; Meng, J.; Guan, Y.; Li, C.; Xiao, C. Identification of a novel inhibitor of isocitrate lyase as a potent antitubercular agent against both active and non-replicating *Mycobacterium tuberculosis*. *Tuberculosis* **2016**, *97*, 38–46.
39. Sharma, V.; Sharma, S.; Hoener zu Bentrup, K.; McKinney, J. D.; Russell, D. G.; Jacobs Jr, W. R.; Sacchettini, J. C. Structure of isocitrate lyase, a persistence factor of *Mycobacterium tuberculosis*. *Nat. Struct. Biol.* **2000**, *7*, 663–668.
40. Shukla, H.; Kumar, V.; Singh, A. K.; Singh, N.; Kashif, M.; Siddiqi, M. I.; Yasoda Krishnan, M.; Sohail Akhtar, M. Insight into the structural flexibility and function of *Mycobacterium tuberculosis* isocitrate lyase. *Biochimie* **2015**, *110*, 73–80.
41. Kitchen, D. B.; Decornez, H.; Furr, J. R.; Bajorath, J. Docking and scoring in virtual screening for drug discovery: methods and applications. *Nat. Rev. Drug Discov.* **2004**, *3*, 935–949.
42. Lavecchia, A.; Di Giovanni, C. Virtual screening strategies in drug discovery: a critical review. *Curr. Med. Chem.* **2013**, *20*, 2839–2860.
43. Lionta, E.; Spyrou, G.; Vassilatis, D. K.; Cournia, Z. Structure-based virtual screening for drug discovery: principles, applications and recent advances. *Curr. Top. Med. Chem.* **2014**, *14*, 1923–1938.
44. InterBioScreen Ltd., 121019 Moscow, P.O. Box 218, Russia. <http://www.ibscreen.com> (accessed August 16, 2017).
45. Jones, G.; Willett, P.; Glen, R. C.; Leach, A. R.; Taylor, R. Development and validation of a genetic algorithm for flexible docking. *J. Mol. Biol.* **1997**, *267*, 727–748.
46. Eldridge, M. D.; Murray, C. W.; Auton, T. R.; Paolini, G. V.; Mee, R. P. Empirical scoring functions: I. The development of a fast empirical scoring function to estimate the binding affinity of ligands in receptor complexes. *J. Comput. Aided Mol. Des.* **1997**, *11*, 425–445.

47. Verdonk, M. L.; Cole, J. C.; Hartshorn, M. J.; Murray, C. W.; Taylor, R. D. Improved protein–ligand docking using GOLD. *Proteins* **2003**, *52*, 609–623.
48. Korb, O.; Stutzle, T.; Exner, T. E. Empirical scoring functions for advanced protein–ligand docking with PLANTS. *J. Chem. Inf. Model* **2009**, *49*, 84–96.
49. Mooij, W.; Verdonk, M. L. General and targeted statistical potentials for protein–ligand interactions. *Proteins* **2005**, *61*, 272–287.
50. Fersht, A. *Structure and mechanism in protein science: a guide to enzyme catalysis and protein folding*; W. H. Freeman and Company: New York, 1999.
51. Oprea, T. I.; Bologa, C.; Olah, M. Compound selection for virtual screening. In *Virtual screening in drug discovery*, Alvarez, J., Shoichet, B. K., Eds.; Taylor & Francis: London, 2005, pp. 89–106.
52. Axerio-Cilies, P.; Castañeda, I. P.; Mirza, A.; Reynisson, J. Investigation of the incidence of “undesirable” molecular moieties for high-throughput screening compound libraries in marketed drug compounds. *Eur. J. Med. Chem.* **2009**, *44*, 1128–1132.
53. Reynisson, J.; O'Neill, C.; Day, J.; Patterson, L.; McDonald, E.; Workman, P.; Katan, M.; Eccles, S. A. The identification of novel PLC-gamma inhibitors using virtual high throughput screening. *Bioorg. Med. Chem.* **2009**, *17*, 3169–3176.
54. Robinson, E.; Leung, E.; Matuszek, A. M.; Krogsgaard-Larsen, N.; Furkert, D. P.; Brimble, M. A.; Richardson, A.; Reynisson, J. Virtual screening for novel Atg5–Atg16 complex inhibitors for autophagy modulation. *Med. Chem Commun.* **2015**, *6*, 239–246.
55. Khomenko, T.; Zakharenko, A.; Odarchenko, T.; Arabshahi, H. J.; Sannikova, V.; Zakharova, O.; Korchagina, D.; Reynisson, J.; Volcho, K.; Salakhutdinov, N. New inhibitors of tyrosyl-DNA phosphodiesterase I (Tdp 1) combining 7-hydroxycoumarin and monoterpenoid moieties. *Bioorg. Med. Chem.* **2016**, *24*, 5573–5581.

56. Huang, R.; Ayine-Tora, D. M.; Muhammad Rosdi, M. N.; Li, Y.; Reynisson, J.; Leung, I. K. H. Virtual screening and biophysical studies lead to HSP90 inhibitors. *Bioorg. Med. Chem. Lett.* **2017**, *27*, 277–281.
57. Zhu, F.; Logan, G.; Reynisson, J. Wine Compounds as a Source for HTS Screening Collections. A Feasibility Study. *Mol. Inf.* **2012**, *31*, 847–855.
58. Savitsky, P.; Bray, J.; Cooper, C. D.; Marsden, B. D.; Mahajan, P.; Burgess-Brown, N. A.; Gileadi, O. High-throughput production of human proteins for crystallization: The SGC experience, *J. Struct. Biol.* **2010**, *172*, 3–13.
59. Gileadi, O.; Burgess-Brown, N. A.; Colebrook, S. M.; Berridge, G.; Savitsky, P.; Smees, C. E. A.; Loppnau, P.; Johansson, C.; Salah, E.; Pantic, N. H. High throughput production of recombinant human proteins for crystallography. In: *Structural proteomics: high-throughput methods*; Kobe, B.; Guss, M.; Huber, T. Eds.; Humana Press: New York, 2008; Chapter 14, pp 221–246.
60. Wu, P. S. C.; Otting, G. Rapid pulse length determination in high-resolution NMR. *J. Magn. Reson.* **2005**, *176*, 115–119.
61. Berman, H.; Henrick, K.; Nakamura, H. Announcing the worldwide Protein Data Bank. *Nat. Struct. Biol.* **2003**, *10*, 980.
62. Berman, H. M.; Westbrook, J.; Feng, Z.; Gilliland, G.; Bhat, T. N.; Weissig, H.; Shindyalov, I. N.; Bourne, P. E. The Protein Data Bank. *Nucl. Acids Res.* **2000**, *28*, 235–242.
63. Allinger, N. L. Conformational analysis. 130. MM2. A hydrocarbon force field utilizing V1 and V2 torsional terms. *J. Am. Chem. Soc.* **1977**, *99*, 8127–8134.
64. Ioakimidis, L.; Thoukydidis, L.; Mirza, A.; Naeem, S.; Reynisson, J. Benchmarking the reliability of QikProp. Correlation between experimental and predicted values. *QSAR & Comb. Sci.* **2008**, *27*, 445–456.

65. Darley, D. J.; Selmer, T.; Clegg, W.; Harrington, R. W.; Buckel, W.; Golding, B. T. Stereocontrolled synthesis of (2*R*,3*S*)-2-methylisocitrate, a central intermediate in the methylcitrate cycle. *Helv. Chim. Acta.* **2003**, *86*, 3991–3999.

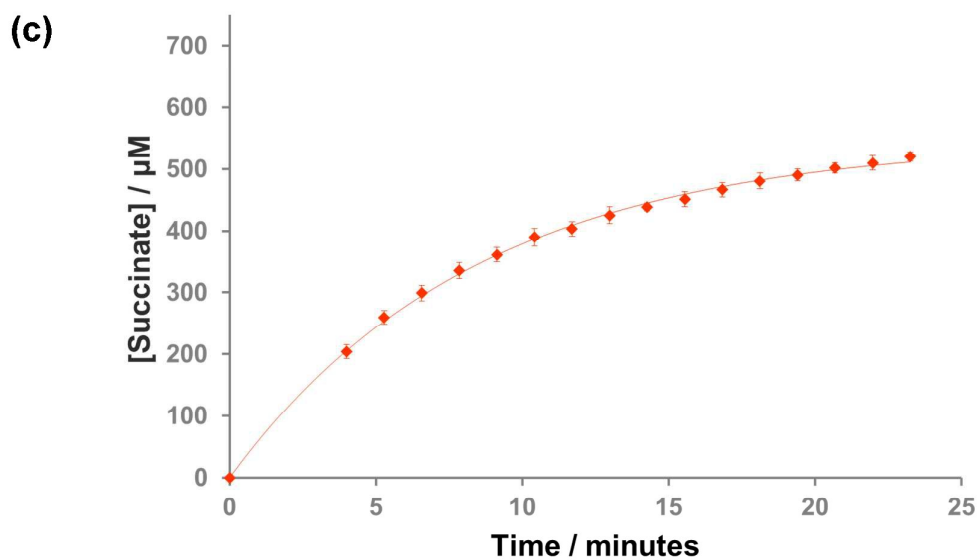
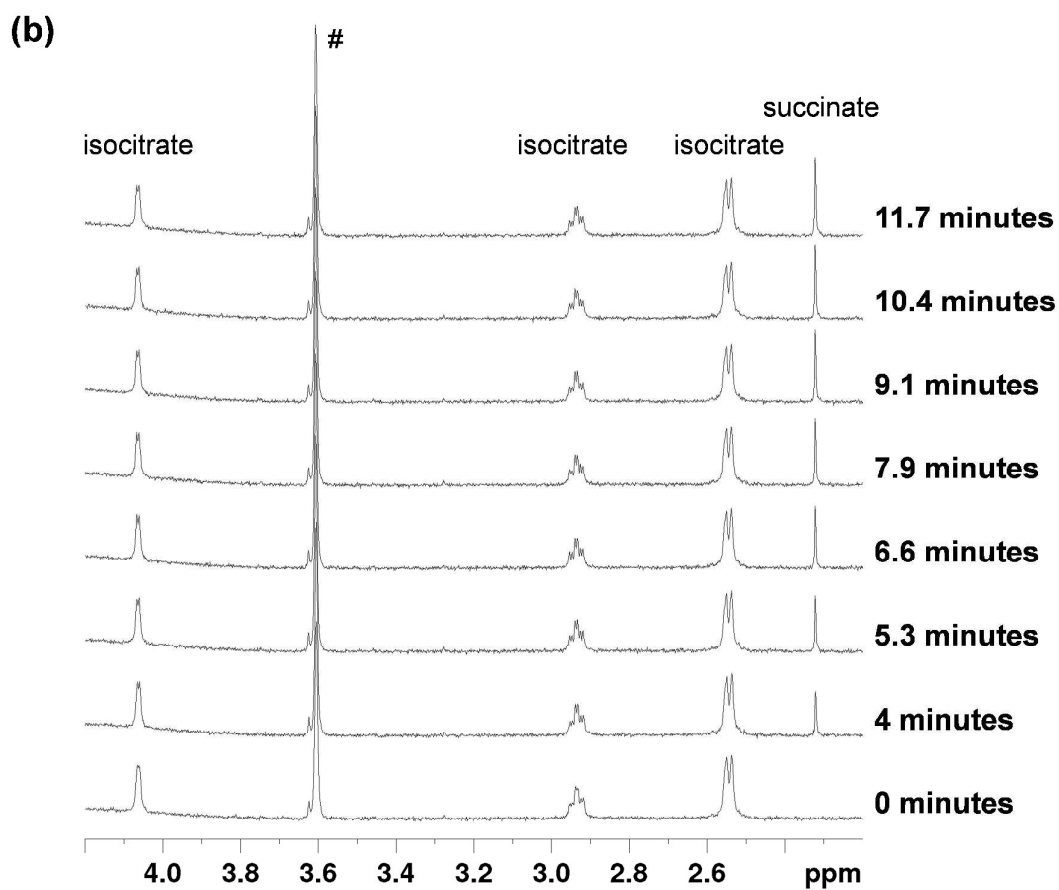
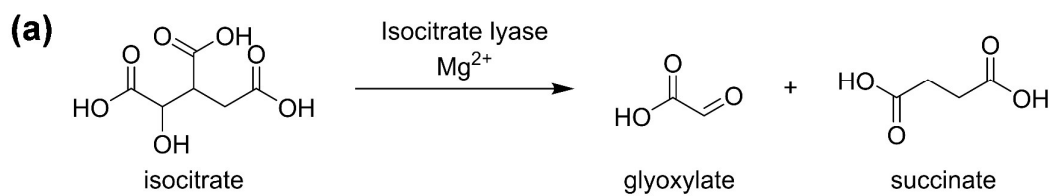


Figure 1: (a) Isocitrate lyase catalyses the conversion of isocitrate to glyoxylate and succinate; (b) ^1H NMR spectroscopy to monitor ICL1-catalysed turnover of isocitrate into succinate; (c) Corresponding plot of the isocitrate turnover data. The curve was added to aid visualisation. Sample contained 190 nM ICL1, 1 mM DL-isocitrate, 5 mM MgCl_2 and 50 mM Tris/Tris- D_{11} (pH 7.5) in 90% H_2O and 10% D_2O . The hashtag (#) indicates Tris/Tris- D_{11} peak. The errors shown are the standard deviation from three separate measurements.

	$K_M / \mu\text{M}$	$k_{\text{cat}} / \text{s}^{-1}$
This study	290 ± 10	4.3 ± 0.1
Gould <i>et al.</i> ¹²	190	5.24

Table 1: Kinetic parameters of ICL1 with DL-isocitrate as substrate. Measurements were made using samples contained 190 nM ICL1, varying concentration of DL-isocitrate, 5 mM MgCl₂ and 50 mM Tris/Tris-D₁₁ (pH 7.5) in 90% H₂O and 10% D₂O. The errors shown are the standard deviation from three separate measurements.

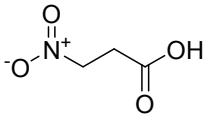
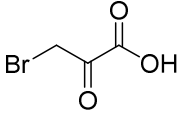
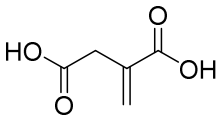
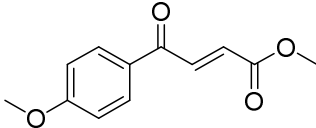
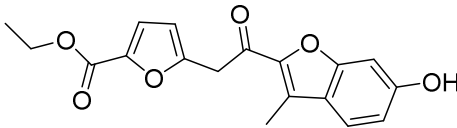
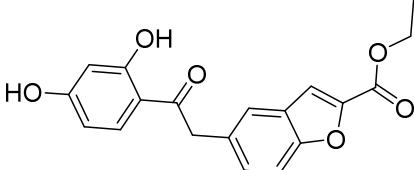
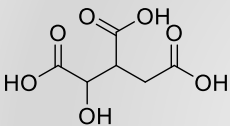
Inhibitor	Structure	IC ₅₀ / μM
3-Nitropropionate		14.7 ± 1.8
3-Bromopyruvate		17.5 ± 1.0
Itaconic acid		29.4 ± 4.1
Methyl-4-(4-methoxyphenyl)-4-oxobut-2-enoate		250 ± 7
Compound 29		>100
Compound 38		>100

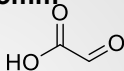
Table 2: IC₅₀ values of ICL1 inhibitors with DL-isocitrate as substrate. Measurements were made using samples contained 190 nM ICL1, 1 mM DL-isocitrate, 5 mM MgCl₂, varying

concentration of inhibitor and 50 mM Tris/Tris-D₁₁ (pH 7.5) in 90% H₂O and 10% D₂O. The errors shown are the standard deviation from three separate measurements. Compounds 29 and 38 were obtained by virtual high-throughput screening (see Supplementary Figures S12–S14).

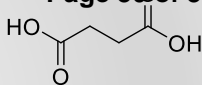


isocitrate

Isocitrate lyase
MedChemComm
 Mg^{2+}

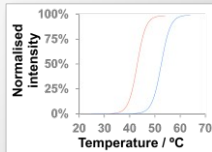
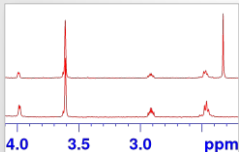


glyoxylate



succinate

NMR
spectroscopy



Thermal
shift assay